Inorganic Chemistry

pubs.acs.org/IC Article

Control of Porphyrin Planarity and Aggregation by Covalent Capping: Bissilyloxy Porphyrin Silanes

Burhan A. Hussein, Zainab Shakeel, Andrew T. Turley, Aisha N. Bismillah, Kody M. Wolfstadt, Julia E. Pia, Melanie Pilkington, Paul R. McGonigal, and Marc J. Adler*

Cite This: https://dx.doi.org/10.1021/acs.inorgchem.0c01891 Read Online

ACCESS | Metrics & More | Article Recommendations | Supporting Information

ABSTRACT: Porphyrins are cornerstone functional materials that are useful in a wide variety of settings, ranging from molecular electronics to biology and medicine. Their applications are often hindered, however, by poor solubilities that result from their extended, solvophobic aromatic surfaces. Attempts to counteract this problem by functionalizing their peripheries have been met with only limited success. Here, we demonstrate a versatile strategy to tune the physical and electronic properties of porphyrins using an axial functionalization approach. Porphyrin silanes (PorSils) and bissilyloxy PorSils (SOPS) are prepared from porphyrins by operationally simple κ^4N-silylation protocols, introducing bulky silyloxy "caps" that are central and perpendicular to the planar porphyrin. While porphyrins typically form either J- or H-aggregates, SOPS do not self-associate in the same manner: the silyloxy axial substituents dramatically improve the solubility by inhibiting aggregation. Moreover, axial porphyrin functionalization offers convenient handles through which optical, electronic, and structural properties of the porphyrin core can be modulated. We observe that the identity of the silyloxy substituent impacts the degree of planarity of the porphyrin in the solid state as well as the redox potentials.

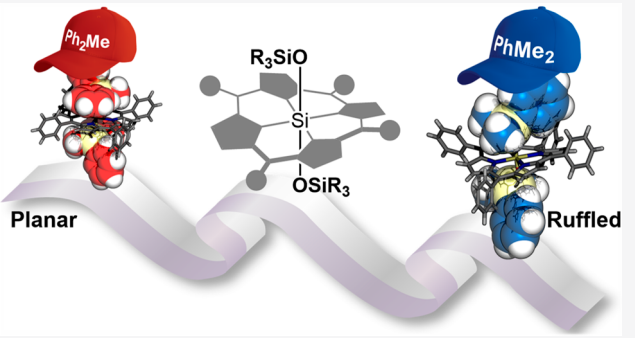

INTRODUCTION

Porphyrins are a long-known and well-studied class of compounds.[1] Naturally occurring variants are vital for the biochemistry of both plants (e.g., chlorophyll, a photoredox catalyst for photosynthesis) and animals (e.g., heme, an oxygen carrier).[2] Accordingly, significant efforts have been dedicated to establishing laboratory syntheses of this class of compounds.[1b,d,3] Both porphyrins and κ^4N,N',N'',N'''-porphyrin–metal complexes (i.e., metalloporphyrins)[4] possess optical, electronic, and chemical properties that make them useful in a range of applied fields, including photodynamic therapy,[5,6] biological imaging,[7] organic photovoltaics,[8] photoredox catalysis,[9] and analytical chemistry.[10] However, their applications can be hindered by their suboptimal physical properties. A constraining drawback of working with porphyrins is that they are difficult to handle and process, owing to their poor solubilities, which can be ascribed to the favorable J- or H-aggregation of their exposed aromatic surfaces.[11] Efforts have been made to prepare derivatives that exhibit improved solubilities in aqueous[12] and organic[13] solutions. The inhibition of aggregation has generally been accomplished through peripheral functionalization of the porphyrin with (i) hydrophilic or nonconjugated lipophilic groups to interact favorably with the solvent medium and/or (ii) bulky groups that sterically disfavor intermolecular association. In nature, porphyrins are buried in biomolecular hydrophobic clefts, which circumvents the solubility obstacle; synthetic systems mimicking this approach have recently been explored to improve photophysical and electrochemical performance.[14]

Phthalocyanines (Pcs)[15] have been used for many of the same applications as porphyrin compounds.[16] Like porphyrins, Pcs are planar and suffer from poor solubilities. However, an elegant approach to improve their physical properties has been to silylate the center of the Pc, introducing axially oriented groups that shield the aromatic surface. Beyond its effect on the solubility, silylation modifies the optical and electronic profiles of Pcs, which has led to over 1000 papers discussing the synthesis, properties, and applications of silylated Pcs (Si-Pcs).[17] Curiously, however, there is a relative dearth of literature (<60 papers) describing such functionalization of the parent porphyrin compounds, which is presumably due to the relatively harsh conditions and operationally complex protocols used to incorporate the central silicon atom. While Si-Pcs are

Received: June 29, 2020

https://dx.doi.org/10.1021/acs.inorgchem.0c01891
Inorg. Chem. XXXX, XXX, XXX−XXX

Scheme 1. Synthesis of the Target Library of Bissilyloxy Porphyrin Silanes (SOPS)[a]

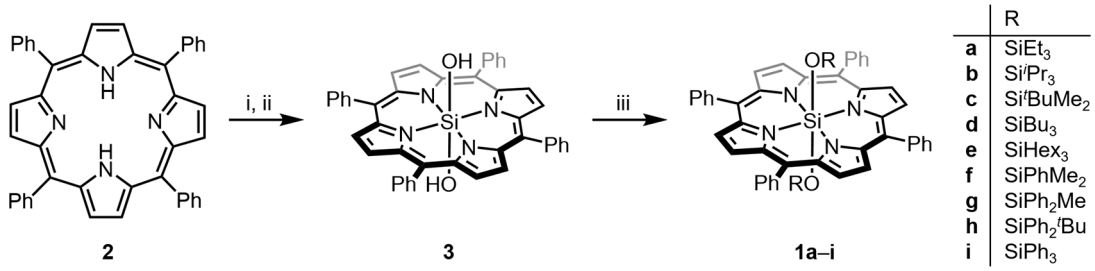

[a]Reagents and conditions: (i) $HSiCl_3$, Et_3N, room temperature (rt), 24 h, 85%; (ii) tetrahydrofuran, water, reflux, 2 h, quantitative; (iii) chlorosilane (RCl), Et_3N, 1,2-dichloroethane, reflux, 16 h, 82−97%.

formed in the presence of $SiCl_4$ to (i) template the macrocyclization and (ii) silylate in situ, porphyrin silanes (PorSils) have been synthesized by first making the porphyrin and then inserting the silicon by forming the $[porphyrin]^{2-}$ species with a strong amide base under strictly anhydrous conditions.[18,19] Sun and co-workers were able to silylate two porphyrins using $HSiCl_3$ and a tertiary amine base. However, purification of the resulting PorSil dichloride requires chromatography on neutral alumina,[20] which makes the protocol too inefficient and expensive to be applied as a general method on a large scale. Furthermore, this protocol can be difficult to reproduce, as the PorSil dichloride can react with the alumina sorbent via nucleophilic substitution of a chloride.

This lack of development of PorSils is unfortunate given that peripheral ring functionalization, allowing for useful tuning of the electronic properties, is much easier to achieve for PorSils than for Si-Pcs. There have been relatively few reports of peripherally functionalized Si-Pcs,[21] as the substituted phthalic acids required as starting materials are synthetically challenging and scarcely commercially available. Porphyrins, on the other hand, possess bridging methines connecting their pyrrole rings that serve as convenient handles for *meso* substitution. This *meso* substitution is readily achieved by simply forming the porphyrin from commercially available aldehydes, of which there are many. Therefore, a robust procedure for κ^4N-silylation of porphyrin derivatives is an appealing target that would provide access to PorSil materials that combine the electronic tuneability of porphyrins with the improved physical properties of Si-Pcs.

Here, we describe a straightforward and general synthetic approach to PorSils (Scheme 1), which has allowed us to elaborate them into a new class of porphyrins, bissilyloxy PorSils (SOPS). Investigation of this series of SOPS (**1a**−**1i**) based on 5,10,15,20-tetraphenylporphyrin (TPP, **2**) revealed that the axial substituents not only serve to solubilize the porphyrin but also to tune their optical and electronic properties.

RESULTS AND DISCUSSION

Synthesis and Reactivity of PorSils and SOPS. Tetraphenylporphyrin (TPP, **2**) was synthesized by the Adler−Longo method.[3b] Previous methodologies for accessing PorSils relied on the use of a highly reactive lithium amide to deprotonate the porphyrin prior to reaction with $HSiCl_3$, which was found to be a better porphyrin-silylating reagent than the perhaps more intuitive building block $SiCl_4$.[18] Sun and co-workers found that porphyrin silylation could be accomplished by combining the porphyrin and $HSiCl_3$ in the presence of Pr_3N.[20] They relied on chromatography to purify the resulting TPP-$Si(Cl)_2$ (**2**-$SiCl_2$), an inefficient approach that also notably did not work in our hands, as the modified porphyrin covalently reacted with the solid support. We accomplished the silylation of **2** using $HSiCl_3$ with Et_3N, a common laboratory reagent (Scheme 1). After aqueous workup, residual Et_3N can be readily removed by evaporation. Using this method we were able to avoid the necessity for chromatography, and instead were able to isolate our desired product by simple liquid−liquid extraction, resulting in up to an 85% yield of **2**-$SiCl_2$. The generalization of this reaction in combination with the simplification of the purification procedure are steps forward for the prospects of developing this class of molecules. To synthesize the SOPS, **2**-$SiCl_2$ was converted quantitively to **3** by refluxing in a THF/water mixture and subsequently silylated using Et_3N and the respective silyl chloride (Scheme 1). These final compounds were air-stable and purified by column chromatography using silica gel and alkaline eluents (see Supporting Information); large scale purification could be accomplished by recrystallization.

It is worth commenting on the more practical aspects of this synthesis, particularly in reference to key intermediate **2**-$SiCl_2$. While stable in open air and during neutral aqueous workup, the Si−Cl bonds in the PorSil are labile enough that a reaction quickly and quantitatively occurs between **2**-$Si(Cl)_2$ and silica gel (in both column and thin-layer chromatography (TLC)). Neither the precursor (**2**) nor subsequent product (**3**) display such reactivity. This allows for facile tracking of the reaction progress in either the generation of **2**-$SiCl_2$ from **2** or consumption of **2**-$SiCl_2$ to make **3**, as **2**-$SiCl_2$ is completely immobile on a silica TLC plate.[22]

NMR Analysis. The NMR spectra of the synthesized SOPS provide insight into the structural and electronic characteristics of these molecules (Figure 1). The ring current of the aromatic porphyrin shields the alkyl/aryl protons of the silyloxy axial substituents, resulting in marked upfield shifts of these signals. This was not unexpected: N−H protons in **2**, which also lie in the shielded porphyrin core, are observed at −2.75 ppm, and similar upfield shifts are observed for axial substituents in related PorSils and SiPcs.[23] This shielding falls off with the distance from the silane (and thus the center of the ring current); for example, in TPP-$Si(OSiPh_3)_2$ (**1i**), the signal for the *ortho* protons (H_E) is visible at 4.69 ppm, significantly upfield from the usual aromatic region, and the signal for the *meta* protons (H_F) is observed at 6.57 ppm (Figure 1). An additional consequence is that, while phenylsilanes typically have overlapping signals for the *meta* (H_F) and *para* (H_G) protons, such protons in these compounds (i.e., **1f**−**1i**) are

https://dx.doi.org/10.1021/acs.inorgchem.0c01891
Inorg. Chem. XXXX, XXX, XXX−XXX

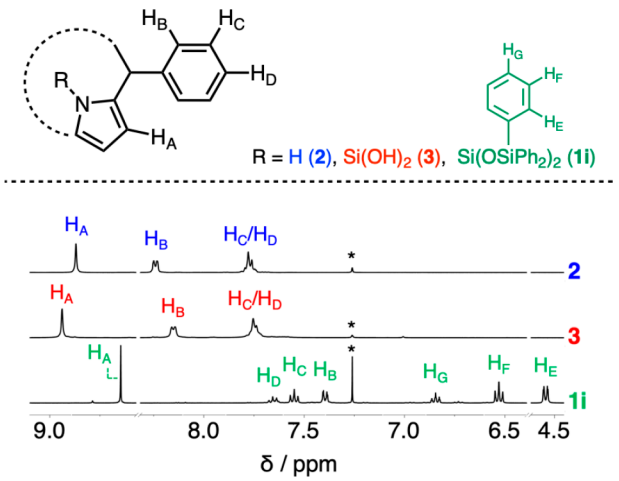

Figure 1. Partial ^{1}H NMR spectra (400 MHz, $CDCl_3$, 298 K) of **2**, **3**, and **1i** showing (i) that aromatic resonances of the axial substituent are shifted upfield by their proximity to the porphyrin ring and (ii) that H_B is shifted significantly upfield in aromatic SOPS (**1i**). *Signal from residual $CHCl_3$ in $CDCl_3$.

completely resolved, with $\Delta\delta$ values of 0.26−0.32 ppm. A similar effect is observed in the ^{13}C NMR spectra, with significant upfield shifts observed for the axial silane substituents (see Supporting Information, Figures S1−18).

While the proton resonance for H_B appears at approximately 8.1−8.2 ppm (Figure 1) in the spectra of **2** and alkyl capped derivatives **1a**−**1e**, it is shifted upfield to 7.4−8.0 ppm for **1f**−**1i**. We attribute this effect to through-space interactions between H_B and the aromatic ring(s) of the capping groups in **1f**−**1i**; such interactions are also observed in the solid state (see Figures S49−53). All NMR spectra acquired at ambient temperatures were well-resolved; this evidence of rapid conformational sampling suggests that these intramolecular contacts do not restrict bond rotation. There is, however, a distinct broadening of the aromatic peaks of the silyloxy cap in **1f** at low temperatures, indicating anisotropy due to slow conformational sampling. We were unable to reach a temperature low enough to sufficiently slow the rate of interconversion such that two distinct species could be detected (see Figure S19).

Impact of Axial Substitution on Porphyrin Planarity. PorSils have previously been observed to have distortion in the planarity of the ring system in the solid state, which is due to the small size of silicon relative to the porphyrin cavity size.[24] In these instances, the porphyrin core slightly contracts to allow for sufficient orbital overlap between the pyrrole nitrogen atoms and the electron-deficient silicon atom. These nonplanar porphyrins[25] can adopt a variety of conformations, including ruffled and waved,[26] which each have characteristic patterns of displacement. Of the 10 previously reported porphyrin silane crystal structures, four were close to planar (Δr < 0.15 Å: TPP-$Si(OH)_2$[27] TPP-$Si(CH_2TMS)_2$, TPP-$Si(CHCH_2)_2$, and TPP-$Si(CCPh)_2$[28]) and six were clearly nonplanar ($\Delta r \gg 0.15$ Å: $[TPP\text{-}Si(THF)_2]^{2+}\cdot 2Cl^-$,[29] TPP-$SiOTf_2$,[18] TPP-SiMePh,[30] TPP-$SiPh_2$,[28] tetrakis(*p*-tolyl)porphyrin-SiF_2, and tetrakis(*p*-trifluoromethylphenyl)porphyrin-SiF_2[31]).

From this set, it seems as though planarity can be achieved if both (i) the axial substituents are sufficiently small so as to not abut the porphyrin and (ii) the axial ligand is capable of π-backbonding to provide the silicon with extra electron density and allow Si−N bonds to lengthen to planarity. For example, while a fluorine atom is certainly small, it does not effectively provide electron density to the silicon via unshared electrons. On the other hand, the phenyl substituents can more readily π-backbond to the silicon; however, the *ortho* hydrogens have a deleterious steric interaction with the macrocyclic ring, preventing porphyrin planarization. This theory is also supported by the observed Si−N and Si−X (X = first atom of axial substituent) bond lengths: planar PorSils feature longer Si−N bonds compared to nonplanar structures, and the Si−X bond lengths are similar to those in tetracoordinate silanes as opposed to the elongated bonds expected in a hexacoordinate silane.[32]

To systematically probe the impact of axial substitution on the solid-state conformation of the PorSils, single crystals of the four species that possessed aromatic silyl caps **1f**−**1i** were analyzed by X-ray diffraction. These data confirmed the presumed structures in all cases: in each of the four structures,

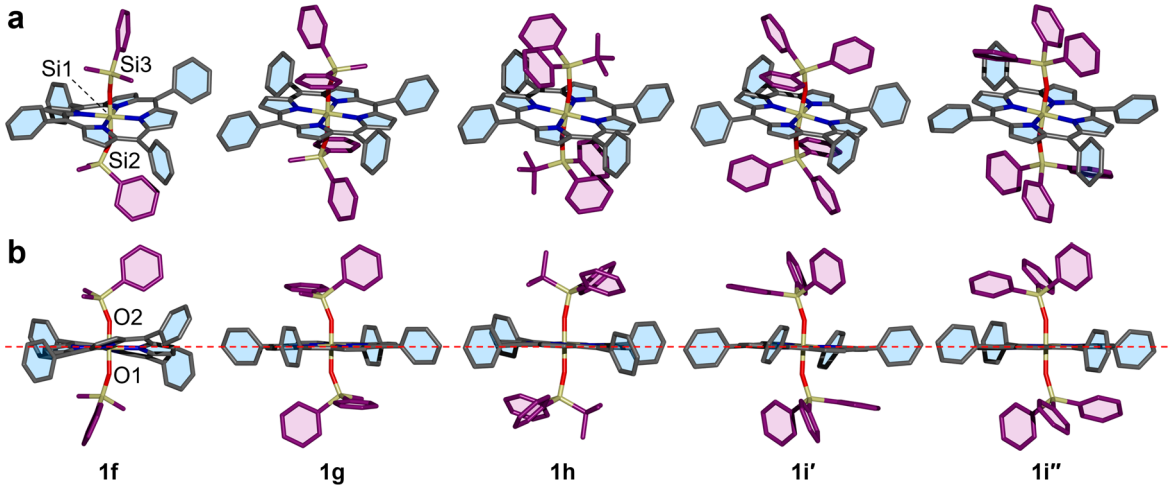

Figure 2. (a) X-ray crystal structures of SOPS **1f**−**1i** confirm the presence and structure of capping groups on either face of the porphyrin units. Both independent molecules in the unit cell of **1i** are shown. (b) Near-linear Si1−O−Si linkages (bond angles 150−168°) connect the bulky silyloxy caps to the PorSil. The porphyrin system of **1f** is ruffled while **1i** is slightly bent. Nitrogen atoms are shown in blue, silicon atoms in yellow, oxygen atoms in red, and carbon atoms in gray and purple. Hydrogen atoms are omitted for clarity.

https://dx.doi.org/10.1021/acs.inorgchem.0c01891
Inorg. Chem. XXXX, XXX, XXX−XXX

Table 1. Selected Data from Crystal Structures of SOPS 1f−1i

compound		Si1−O bond lengths[a] (Å)	Si1−O−Si bond angles[a] (deg)	Δr[b] (Å)	displacement of individual *meso* carbons from N1−Si1−N2 plane[a,b] (Å)
TPP−Si($OSiMe_2Ph$)$_2$ (**1f**)		1.688(2) (Si1−O1) 1.681(2) (Si1−O2)	150.8(2) (Si1−O1−Si2) 155.2(2) (Si1−O2−Si3)	0.469	−0.431 (C5), + 0.507 (C16), −0.549 (C27), + 0.389 (C38)
TPP−Si($OSiMePh_2$)$_2$ (**1g**)		1.6758(14)	157.75(10)	0.006	0 (C5), + 0.011 (C16), 0 (C5), −0.011 (C16)
TPP−Si($OSiPh_2{}^t$Bu)$_2$ (**1h**)		1.6801(12)	167.57(9)	0.111	−0.152 (C5), −0.069 (C16), +0.152, (C5), + 0.069 (C16)
TPP−Si($OSiPh_3$)$_2$ (**1i**)	pose 1[c] (**1i′**)	1.684(3)	163.9(2)	0.058	−0.006 (C5), −0.109 (C16), +0.006 (C5), + 0.109 (C16)
	pose 2[c] (**1i″**)	1.690(3)	159.8(2)	0.085	−0.025 (C45), −0.145 (C56), +0.025 (C45), + 0.145 (C56)

[a]Atoms labeled according to designation in the crystal structure: Si1 is the central silicon atom; Si2 and Si3 are the silicon atoms in the silyloxy caps; and O1 and O2 are the linking oxygens of the bissilyl ethers. N1 and N2 refer to two *cis*-coordinated nitrogens. For full numbering scheme, see Figures S41, S43, S45, and S47. [b]See ref 25; (+) and (−) designations represent relative orientation. [c]The asymmetric unit in **1i** contains two molecules, each in a different conformational pose (**1i′** and **1i″**).

the hypercoordinate silicon core adopts an octahedral structure with the two silyloxy ligands observed in a *trans* (diaxial) arrangement (Figure 2).

Of the four compounds we examined (seen in Table 1), all deviated from planarity. Compound **1g** is the most planar molecule with two *meso* carbon atoms located *trans* to each other that are displaced above and below the plane by ±0.011 Å. This is the most planar porphyrin silane crystal structure reported to date. The *meso* carbons in **1h** and in both poses of **1i** were each out of plane, but only slightly (≤0.152 Å), and porphyrins maintained overall symmetry around the central silicon. Unique among the studied set, compound **1f** displayed the least planar structure and was surprisingly devoid of symmetry around the central silicon atom. In general, we were gratified to see that modification of the easily incorporated axial silyloxy substituents can control the degree to which the porphyrin deviates from planarity in the crystal structure. This demonstrates that axial substitution is a powerful tool for control of solid-state porphyrin conformation.

In terms of electronics, the iterative replacement of methyl for phenyl groups on the silyloxy cap (**1f** to **1g** to **1i**) should increase the electron density on the silane, allowing for lengthening of the O1−Si2/O2−Si3 bond (Figure 2); the excess electron density on the oxygen could translate to a shorter Si1−O distances and allow the Si−N bonds to lengthen to accommodate the preferred return to planarity of the ring. No such effect is observed. From a sterics perspective, the Si1−O−Si bond angle of the least planar porphyrin (**1f**) is the most acute, so one might think the steric interaction is influencing the ring structure; however, (i) this is also the smallest of the studied substituents and sterically arranged in the least impacting way in the solid state (with the phenyl pointing away from the porphyrin), and (ii) there is no general correlation between that bond angle and planarity in the studied compounds.

There does appear to be a correlation between the axial silyloxy substituent size and Si1−O−Si angle, tending toward linear as the cap size increases in this set. The SOPS bearing the largest substituent (OSi^tBuPh_2, **1h**) displays a remarkably wide bond angle of 168°. The Si1−O bond length also varies based on the silyl cap, though no clear trend is observed. While shorter Si1−O bond distances would be expected in the more planar SOPS, there is a complex interplay among these derivatives with respect to the steric and electronic demands of the silyloxy cap substituents. From this perspective, the Me_2Ph derivative (**1f**) is unique among PorSils that have been examined by X-ray crystallography: it has an Si−X bond distance similar to that of a tetracoordinate silane, yet the porphyrin in the crystal structure is still highly ruffled. The other derivatives seem to fit into the construct derived from previous studies of porphyrin silanes (as discussed above).

One last interesting note is that, while the silyloxy substituents in **1g**, **1h**, and **1i** are arranged in an *anti* configuration with respect to the Si−O(−Si1−)O−Si bond, the highly ruffled **1f** has a Si−O(−Si1−)O−Si dihedral angle of 86.72°. This may be a consequence of the unique conformation of this PorSil, or it could be that the packing in the crystal lattice impacts this arrangement.

Influence of Axial Substitution on Solubility. Owing to its large, three-dimensional hydrophobic surfaces, SOPS (**1a**−**1i**) have a much greater solubility in organic solvents than TPP (**2**), as seen in Table 2. There were also noticeable differences

Table 2. Solubility of TPP (2), Aliphatic SOPS (1e), and Aromatic SOPS (1h)

solvent	limiting concentration[a] (mM)		
	2	**1e**	**1h**
hexanes	0.0[b]	8.0	1.7
toluene	2.5	7.3	4.4
dichloromethane	4.7	13	6.5
ethyl acetate	0.41	6.7	1.2
acetonitrile	0.20	0.05	0.05
ethanol	0.11	0.70	0.28

[a]Limiting concentration determined by titrating 0.1 mL aliquots of a solvent into samples of the porphyrins (5−15 mg) followed by sonication until full dissolution. [b]No dissolution observed up to 10 mg in 15 mL.

in the solubility between the series of aliphatic SOPS and the series of aromatic SOPS; these differences were used to our advantage in the purification process (see Supporting Information). The improved solubilities of the SOPS compared to **2** can be rationalized by considering the noncovalent interactions between the molecules in the solid state. Porphyrins that lack axial capping groups, such as **2**, are known to experience favorable face-to-face aromatic interactions between their large, exposed π-surfaces. These interactions cause aggregation, which in turn can red-shift

https://dx.doi.org/10.1021/acs.inorgchem.0c01891
Inorg. Chem. XXXX, XXX, XXX−XXX

absorption and quench fluorescence. On the other hand, the analysis of the packing structures of **1f**–**1i** (see Figures S42, S44, S46, and S48) shows that the bulky axial caps prevent this interaction. As an illustrative example, there are three molecules near the axial cap of **1h** (Figure 3), but none

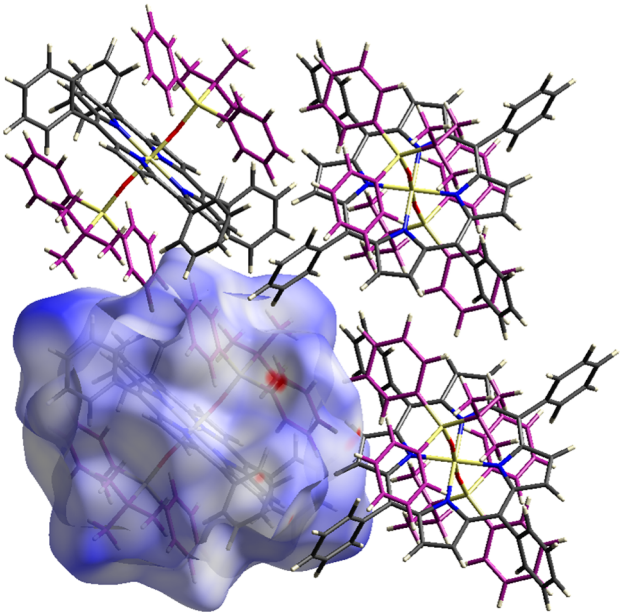

Figure 3. Solid-state superstructure of **1h**, which shows that the silyloxy cap shields the porphyrin core from intermolecular aromatic interactions. A Hirshfeld surface plot reveals that the interatomic distances between neighboring molecules are almost entirely at (white) or above (blue) the sum of the van der Waals radii. Close contacts shown in red.

come into close contact with the surface of the porphyrin ring system itself; they contact the cap instead. A Hirshfeld surface plot[33] of **1h** (Figure 3) and interaction energy calculations (see Tables S3–12 and Figures S56–70) confirm that these interactions between the neighboring molecules are dominated by van der Waals forces. The SOPS contact one another at distances that correspond closely to the sum of the respective van der Waals radii, as can be seen by the large areas of white in the Hirshfeld surface.

Impact of Axial Substitution on Optoelectronic Properties. As expected, all the investigated porphyrins are UV-active compounds (Table 3, Figures 4 and 5a). Silylation

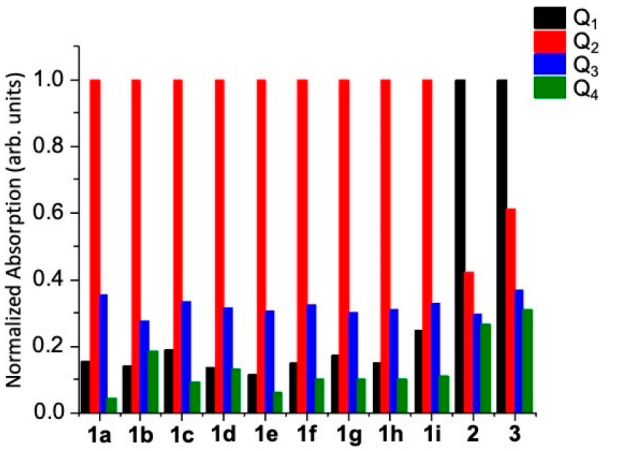

Figure 4. Comparison of normalized absorption forfor 100 mM dichloromethane solutions of **1a**–**1i**, **2**, and **3**.

of TPP (**2**) to make TPP-Si(OH)$_2$ (**3**) does not significantly impact observed λ_{max} values, but there is a small general red-shift, and a J-aggregation-type Soret band[34] is observed around 450 nm. Q_1 is the strongest Q-band of both **2** and **3**, indicating that the dissymmetry that exists in **2** giving rise to this optical phenomenon is also present in **3**. This spectral feature lies in stark contrast to what is typically seen in two-dimensional metalated (i.e., Zn(II), Ni(II), Cu(II), and Fe(II)) porphyrins, which have only one or two Q-bands (with Q_2 and/or Q_3 persisting) due to higher levels of symmetry.[35] Interestingly, when the silyloxy caps are installed we observe Q-band structures more like the metalated porphyrins, with Q_2 being the most intense (Figure 4). There is some differentiation among the relative molar extinction coefficients of the Q bands for SOPS; for example, **1a** has almost no Q_4 band, while **1b** has a Q_4 band that is greater in intensity than Q_1. Notably, in all SOPS, some degree of dissymmetry is evidenced by the presence of all four Q bands, and the respective λ_{max} (Soret and Q bands) values of the SOPS are generally red-shifted compared to that of **2**, with the notable exception of Q_4

Table 3. Physicochemical Data of Studied Porphyrins

	absorption[a] λ_{max} [nm] ($\varepsilon \times 10^{-3}$ [$M^{-1}cm^{-1}$])						$E_{1/2}$[b] [V vs NHE]	
compound	soret	Q_1	Q_2	Q_3	Q_4	emission λ_{max} [nm] (λ_{ex} [nm])	oxidation	reduction
1a	421 (463)	513 (2.91)	552 (18.9)	589 (6.69)	625 (0.87)	605, 643 (430)	1.33	−1.06
1b	422 (510)	512 (2.88)	550 (20.1)	591 (5.48)	623 (3.77)	592, 627 (430)	1.36	−1.21
1c	418 (422)	512 (3.31)	549 (17.4)	586 (5.75)	618 (1.69)	605, 646 (427)	1.34	−1.08
1d	424 (391)	514 (2.90)	555 (17.2)	596 (4.25)	627 (2.78)	598, 645 (424)	1.32	−1.18
1e	423 (425)	514 (3.03)	555 (16.6)	595 (4.73)	627 (1.55)	602, 649 (423)	1.32	−1.35
1f	423 (521)	514 (2.80)	552 (18.8)	591 (6.06)	628 (1.89)	605, 649 (427)	1.35	−1.10
1g	422 (215)	514 (2.88)	553 (19.6)	592 (5.47)	628 (1.24)	600, 648 (423)	1.36	−1.08
1h	423 (415)	512 (2.54)	550 (16.9)	587 (5.21)	628 (1.73)	607, 648 (431)	1.35	−1.11
1i	425 (351)	515 (4.04)	553 (16.2)	592 (5.29)	633 (1.80)	602, 645 (427)	1.33	−1.13
2	417 (519)	514 (18.3)	549 (7.75)	590 (5.39)	646 (4.85)	650, 711 (418)	1.34[c]	−0.92
3	418 (430) 446 (26)	514 (14.0)	550 (8.59)	590 (5.14)	649 (4.33)	600, 650, 711 (418)	1.52	−0.93

[a]Low-energy visible transitions from UV–vis in dichloromethane. [b]Data collected using 0.1 M NBu_4PF_6 dichloromethane solutions at 100 mV s^{-1} and referenced to a ferrocene ($[Fc]/[Fc]^+$) internal standard followed by conversion to NHE; $[Fc]/[Fc]^+$ = +765 mV vs NHE in dichloromethane. [c]A second oxidation peak was observed for **2** at 1.63 V vs NHE.

https://dx.doi.org/10.1021/acs.inorgchem.0c01891
Inorg. Chem. XXXX, XXX, XXX–XXX

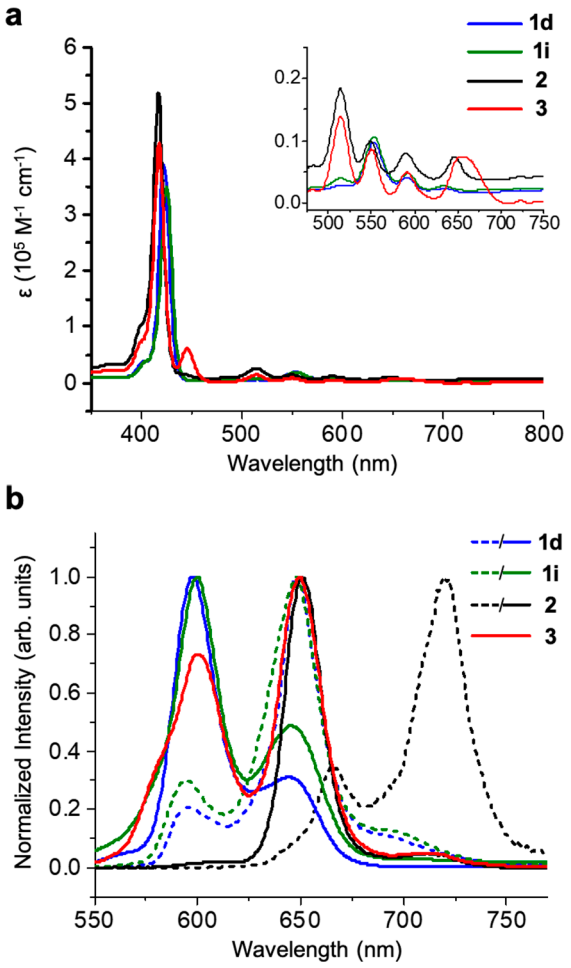

Figure 5. Absorption and emission spectra of a representative set of porphyrins in dichloromethane: **1d** (aliphatic SOPS), **1i** (aromatic SOPS), **2**, and **3**. (a) Absorption spectra of porphyrins, with an inset zoom on the Q bands. (b) Normalized emission profiles of porphyrins (i) in dichloromethane (10 μM, solid lines) and (ii) dispersed in optically clear amorphous polymer films (0.1 wt % ZEONEX film, dotted lines).

(Table 3). Both of these observations can be attributed to the likely ruffling of the porphyrin in solution.[36] This hypothesis is supported by a density functional theory structural study (M06-2X/6-31G with a polarizable continuum model for dichloromethane solvent) that shows nonplanarity in the calculated ground state minimized structure of SOPS in solution (see Figures S54 and S55). Variance among the SOPS λ_{max} values (Soret and Q bands) is modest (Table 3); the largest range can be seen in Q_4, where the lowest (TPP-Si(OSi^tBuMe_2)$_2$, **1c**) and highest (TPP-Si($OSiPh_3$)$_2$, **1i**) λ_{max} values are separated by 15 nm (618 and 633 nm, respectively). These absorption data demonstrate that the selection of a particular silyloxy cap can be used to control the structure of the porphyrin ring. Beer's plots up to a concentration of 100 μM were linear, which confirms that SOPS did not aggregate at the examined concentrations (see Figures S21–29).

The examined porphyrins were fluorescent as dichloromethane solutions (Table 3 and Figure 5b). For **2**, we observed a very strong emission band at 650 nm and a much smaller emission at 711 nm. This two-emission profile is typical of porphyrins and is attributed to two tautomeric states.[37] In toluene, **2** has the same λ_{max} as in dichloromethane but emits relatively more intensely at 711 nm.[38] This demonstrates that environmental effects (i.e., solvent) impact the population distribution of the two tautomers but not the energy of the individual highest occupied molecular orbital–lowest unoccupied molecular orbital (HOMO–LUMO) gaps. When the SOPS (**1a**–**1i**) were excited at their respective Soret bands in solution, two emission signals were noted: one around 600 nm and another closer to 650 nm (Table 3 and Figure 5b). The ∼50 nm blue shift of the SOPS with respect to **2** corresponds to what is seen in fluorescent metalloporphyrins such as TPP-Zn.[39] Interestingly, **3** fluoresces at three distinct λ_{max} values: 600, 650, and 711 nm. This finding suggests that compound **3** (i) possesses an optical character similar to both the free base and metalloporphyrin and/or (ii) has an additional red-shifted emission due to aggregation. The population distribution between the emission bands at ∼600 and ∼650 nm differs from that seen in the SOPS. It is clear that the silyloxy cap is impacting ring electronics, perhaps as a consequence of inhibition of aggregation and/or influence on porphyrin planarity.

Samples of **2**, aliphatic SOPS **1d**, and aromatic SOPS **1i** were also embedded into a ZEONEX polymer matrix and examined by fluorescence (Figure 5b). The emission spectrum of **2** was significantly red-shifted in the ZEONEX film. Given that general environmental effects do not cause such a phenomenon in **2**, this appears to be evidence of aggregation of the porphyrin in the polymer.[40] While SOPS showed an altered population distribution of the two tautomeric states (evidenced by a change in relative intensities of the two emission bands), the energies of these transitions were not affected. These findings support our hypothesis that silyloxy caps discourage aggregation.

The electrochemical behavior of these compounds was studied using cyclic voltammetry (CV) for the full range of synthesized SOPS (Table 3; for CV spectra, see Figures S35–40). All SOPS underwent a reversible one-electron oxidation with similar oxidizing potentials regardless of the identity of the silyloxy cap. However, the SOPS have slightly higher oxidation potentials (1.31–1.35 V) than those observed for **2** (1.31 V) and significantly lower than that observed for **3** (1.52 V). This increase in the oxidation potential indicates a stabilization of the HOMO of the PorSils in solution.

There was more variance in the reduction potential of the SOPS, with values ranging from −1.35 (**1e**) to −1.06 V (**1a**). In all cases, the SOPS were reduced at potential greater than either **2** or **3**, which we observed as −0.92 and −0.93 V, respectively. A small trend was observed for the C_3-symmetrical linear trialkylsilyloxy caps (**1a**, **1d**, and **1e**), with longer chain lengths being associated with reduction potentials of greater magnitudes; this could be due to electron repulsion by the silyloxy substituents. No other obvious trends were observed; however it is clear that the LUMO energies of the SOPS are sensitive to the identity of the silyloxy cap.

CONCLUSIONS AND OUTLOOK

Edge-functionalized porphyrin derivatives are reliable and widely used building blocks for functional organic materials. We have demonstrated that the straightforward, high-yielding modification of porphyrins at their core is a viable alternative way to tune their properties. By silylating the porphyrin and capping with axial silyloxy substituents, we have increased porphyrin solubility and prevented aggregation-induced physicochemical phenomena. The identity of the silyloxy cap

https://dx.doi.org/10.1021/acs.inorgchem.0c01891
Inorg. Chem. XXXX, XXX, XXX–XXX

can be used to tune porphyrin planarity and molecular orbital energies. This approach offers opportunities for the customization of porphyrins through axial tuning and an improvement in the processability of porphyrins via increased solubility.

■ ASSOCIATED CONTENT

Supporting Information

The Supporting Information is available free of charge at https://pubs.acs.org/doi/10.1021/acs.inorgchem.0c01891.

Experimental and synthetic details; ^{1}H, ^{13}C, and variable-temperature NMR spectra; UV−vis, fluorescence, and CV spectra; X-ray crystallographic data and Hirshfeld analysis; density functional theory structural studies; Hirshfeld surfaces brief description; mass spectra (PDF)

Accession Codes

CCDC 1977452−1977455 contain the supplementary crystallographic data for this paper. These data can be obtained free of charge via www.ccdc.cam.ac.uk/data_request/cif, by emailing data_request@ccdc.cam.ac.uk, or by contacting The Cambridge Crystallographic Data Centre, 12 Union Road, Cambridge CB2 1EZ, UK; fax: +44 1223 336033.

■ AUTHOR INFORMATION

Corresponding Author

Marc J. Adler − *Department of Chemistry & Biology, Ryerson University, Toronto, Ontario M5B 2K3, Canada;* orcid.org/0000-0002-1049-509X; Email: marcjadler@ryerson.ca

Authors

Burhan A. Hussein − *Department of Chemistry & Biology, Ryerson University, Toronto, Ontario M5B 2K3, Canada; Department of Chemistry, Durham University, Durham DH1 3LE, United Kingdom*

Zainab Shakeel − *Department of Chemistry & Biology, Ryerson University, Toronto, Ontario M5B 2K3, Canada*

Andrew T. Turley − *Department of Chemistry, Durham University, Durham DH1 3LE, United Kingdom*

Aisha N. Bismillah − *Department of Chemistry, Durham University, Durham DH1 3LE, United Kingdom; Department of Chemistry, Dartmouth College, Hanover, New Hampshire 03755, United States*

Kody M. Wolfstadt − *Department of Chemistry & Biology, Ryerson University, Toronto, Ontario M5B 2K3, Canada*

Julia E. Pia − *Department of Chemistry & Biology, Ryerson University, Toronto, Ontario M5B 2K3, Canada*

Melanie Pilkington − *Department of Chemistry, Brock University, St. Catharines, Ontario L2S 3A1, Canada;* orcid.org/0000-0002-9274-8512

Paul R. McGonigal − *Department of Chemistry, Durham University, Durham DH1 3LE, United Kingdom*

Complete contact information is available at: https://pubs.acs.org/10.1021/acs.inorgchem.0c01891

Author Contributions

The manuscript was written through contributions of all authors.

Notes

The authors declare no competing financial interest.

■ ACKNOWLEDGMENTS

The authors would like to thank Ryerson University for funding. B.A.H. acknowledges the Engineering and Physical Sciences Research Council (EPSRC) Centre for Doctoral Training in Soft Matter and Functional Interfaces (SOFI) for a PhD studentship. A.T.T. and A.N.B. acknowledge EPSRC Doctoral Training Grants. M.P. acknowledges NSERC RTI for support. The authors also thank Bryan Koivisto and Stefania Impellizzeri (Ryerson University) for advice and support.

■ REFERENCES

(1) (a) Sessler, J. L.; Seidel, D. Synthetic Expanded Porphyrin Chemistry. *Angew. Chem., Int. Ed.* **2003**, *42* (42), 5134−75. (b) Vicente, M.; Smith, K. Syntheses and Functionalizations of Porphyrin Macrocycles. *Curr. Org. Synth.* **2014**, *11* (1), 3−28. (c) Day, N. U.; Wamser, C. C.; Walter, M. G. Porphyrin Polymers and Organic Frameworks. *Polym. Int.* **2015**, *64* (7), 833−57. (d) Hiroto, S.; Miyake, Y.; Shinokubo, H. Synthesis and Functionalization of Porphyrins through Organometallic Methodologies. *Chem. Rev.* **2017**, *117* (4), 2910−3043. (e) Mahmood, A.; Hu, J. Y.; Xiao, B.; Tang, A.; Wang, X.; Zhou, E. Recent Progress in Porphyrin-Based Materials for Organic Solar Cells. *J. Mater. Chem. A* **2018**, *6* (35), 16769−16797.

(2) Giovannetti, R. The Use of Spectrophotometry UV−Vis for the Study of Porphyrins. In *Macro to Nano Spectroscopy*; IntechOpen, 2012; Vol. *1*, pp 87−108.

(3) (a) Rothemund, P. A New Porphyrin Synthesis. The Synthesis of Porphin. *J. Am. Chem. Soc.* **1936**, *58*, 625−627. (b) Adler, A. D.; Longo, F. R.; Finarelli, J. D.; Goldmacher, J.; Assour, J.; Korsakoff, L. A Simplified Synthesis for Meso-Tetraphenylporphine. *J. Org. Chem.* **1967**, *32* (2), 476. (c) Lindsey, J. S.; Schreiman, I. C.; Hsu, H. C.; Kearney, P. C.; Marguerettaz, A. M. Rothemund and Adler-Longo Reactions Revisited: Synthesis of Tetraphenylporphyrins under Equilibrium Conditions. *J. Org. Chem.* **1987**, *52* (5), 827−836.

(4) (a) Costas, M. Selective C−H Oxidation Catalyzed by Metalloporphyrins. *Coord. Chem. Rev.* **2011**, *255* (23−24), 2912−2932. (b) Shanmugam, S.; Xu, J.; Boyer, C. Exploiting Metalloporphyrins for Selective Living Radical Polymerization Tunable over Visible Wavelengths. *J. Am. Chem. Soc.* **2015**, *137* (28), 9174−9185. (c) Huang, X.; Groves, J. T. Oxygen Activation and Radical Transformations in Heme Proteins and Metalloporphyrins. *Chem. Rev.* **2018**, *118* (5), 2491−2553.

(5) Kou, J.; Dou, D.; Yang, L. Porphyrin Photosensitizers in Photodynamic Therapy and its Applications. *Oncotarget.* **2017**, *8* (46), 81591−81603.

(6) (a) Dougherty, T. J.; Kaufman, J. E.; Goldfarb, A.; Weishaupt, K. R.; Boyle, D. G.; Mittelman, M. Photoradiation Therapy for the Treatment of Malignant Tumors. *Cancer Res.* **1978**, *38* (8), 2628−2635. (b) Santoro, A. M.; Lo Giudice, M. C.; D'Urso, A.; Lauceri, R.; Purrello, R.; Milardi, D. Cationic Porphyrins are Reversible Proteasome Inhibitors. *J. Am. Chem. Soc.* **2012**, *134* (25), 10451−10457.

(7) (a) Shi, J.; Liu, T. W. B.; Chen, J.; Green, D.; Jaffray, D.; Wilson, B. C.; Wang, F.; Zheng, G. Transforming a Targeted Porphyrin Theranostic Agent into a PET Imaging Probe for Cancer. *Theranostics* **2011**, *1*, 363−370. (b) Huynh, E.; Leung, B. Y.; Helfield, B. L.; Shakiba, M.; Gandier, J. A.; Jin, C. S.; Master, E. R.; Wilson, B. C.; Goertz, D. E.; Zheng, G. In Situ Conversion of Porphyrin Microbubbles to Nanoparticles for Multimodality Imaging. *Nat. Nanotechnol.* **2015**, *10* (4), 325−332. (c) Varchi, G.; Foglietta, F.; Canaparo, R.; Ballestri, M.; Arena, F.; Sotgiu, G.; Guerrini, A.; Nanni, C.; Cicoria, G.; Cravotto, G.; Fanti, S.; Serpe, L. Engineered Porphyrin Loaded Core-Shell Nanoparticles for Selective Sonodynamic Anticancer Treatment. *Nanomedicine* **2015**, *10* (23), 3483−3494.

(8) (a) Martinez-Diaz, M. V.; de la Torre, G.; Torres, T. Lighting Porphyrins and Phthalocyanines for Molecular Photovoltaics. *Chem.*

https://dx.doi.org/10.1021/acs.inorgchem.0c01891
Inorg. Chem. XXXX, XXX, XXX−XXX

Commun. **2010**, *46* (38), 7090−7108. (b) Walter, M. G.; Rudine, A. B.; Wamser, C. C. Porphyrins and Phthalocyanines in Solar Photovoltaic Cells. *J. Porphyrins Phthalocyanines* **2010**, *14* (9), 759−792. (c) Li, L.-L.; Diau, E. W.-G. Porphyrin-Sensitized Solar Cells. *Chem. Soc. Rev.* **2013**, *42* (1), 291−304.

(9) (a) Eriksson, K.; Göthelid, E.; Puglia, C.; Bäckvall, J.; Oscarsson, S. Performance of a Biomimetic Oxidation Catalyst Immobilized on Silica Particles. *J. Catal.* **2013**, *303*, 16−21. (b) Sheng, W.; Jiang, Q.; Luo, W.; Guo, C. Oxidative Rearrangement of Internal Alkynes to Give One-Carbon-Shorter Ketones via Manganese Porphyrins Catalysis. *J. Org. Chem.* **2013**, *78* (11), 5691−5693. (c) Rybicka-Jasinska, K.; Shan, W.; Zawada, K.; Kadish, K. M.; Gryko, D. Porphyrins as Photoredox Catalysts: Experimental and Theoretical Studies. *J. Am. Chem. Soc.* **2016**, *138* (47), 15451−15458. (d) Rybicka-Jasinska, K.; Konig, B.; Gryko, D. Porphyrin-Catalyzed Photochemical C−H Arylation of Heteroarenes. *Eur. J. Org. Chem.* **2017**, *2017*, 2104−2107.

(10) Biesaga, M.; Pyrzynska, K.; Trojanowicz, M. Porphyrins in Analytical Chemistry. A Review. *Talanta* **2000**, *51* (2), 209−224.

(11) White, W. I. Aggregation of Porphyrins and Metalloporphyrins. In *The Porphyrins*; Dolphin, D., Ed.; Elsevier Inc.: New York, NY, 1978; Vol. *5*, pp 303−339.

(12) (a) Murashima, T.; Tsujimoto, S.; Yamada, T.; Miyazawa, T.; Uno, H.; Ono, N.; Sugimoto, N. Synthesis of Water-Soluble Porphyrin and the Corresponding Highly Planar Benzoporphyrin without Meso-Substituents. *Tetrahedron Lett.* **2005**, *46* (1), 113−116. (b) Ruzié, C.; Even, P.; Boitrel, B. Dioxygen Binding of Water-Soluble Iron(II) Porphyrins in Phosphate Buffer at Room Temperature. *Org. Biomol. Chem.* **2007**, *5* (10), 1601−1604. (c) Remello, S. N.; Kuttassery, F.; Hirano, T.; Nabetani, Y.; Yamamoto, D.; Onuki, S.; Tachibana, H.; Inoue, H. Synthesis of Water-Soluble Silicon-Porphyrin: Protolytic Behaviour of Axially Coordinated Hydroxy Group. *Dalton Trans.* **2015**, *44* (46), 20011−20020.

(13) (a) Paine, J. B.; Kirshner, W. B.; Moskowitz, D. W.; Dolphin, D. Improved Synthesis of Octaethylporphyrin. *J. Org. Chem.* **1976**, *41* (24), 3857−3860. (b) Thamyongkit, P.; Speckbacher, M.; Diers, J. R.; Kee, H. L.; Kirmaier, C.; Holten, D.; Bocian, D. F.; Lindsey, J. S. Swallowtail Porphyrins: Synthesis, Characterization and Incorporation into Porphyrin Dyads. *J. Org. Chem.* **2004**, *69* (11), 3700−3710. (c) Oda, K.; Akita, M.; Hiroto, S.; Shinokubo, H. Silylethynyl Substituents as Porphyrin Protecting Groups for Solubilization and Selectivity Control. *Org. Lett.* **2014**, *16* (6), 1818−1821.

(14) (a) Liu, C.; Liu, K.; Wang, C.; Liu, H.; Wang, H.; Su, H.; Li, X.; Chen, B.; Jiang, J. Elucidating Heterogeneous Photocatalytic Superiority of Microporous Porphyrin Organic Cage. *Nat. Commun.* **2020**, *11* (1), 1047. (b) Liu, W.; Lin, C.; Weber, J. A.; Stern, C. L.; Young, R. M.; Wasielewski, M. R.; Stoddart, J. F. Cyclophane-Sustained Ultrastable Porphyrins. *J. Am. Chem. Soc.* **2020**, *142* (19), 8938.

(15) Sakamoto, K.; Ohno-Okumura, E. Syntheses and Functional Properties of Phthalocyanines. *Materials* **2009**, *2* (3), 1127−1179.

(16) (a) Xue, J.; Uchida, S.; Rand, B.; Forrest, S. 4.2% Efficient Organic Photovoltaic Cells with Low Series Resistances. *Appl. Phys. Lett.* **2004**, *84*, 3013−3015. (b) Kim, D. Y.; So, F.; Gao, Y. Aluminum Phthalocyanine Chloride/C_{60} Organic Photovoltaic Cells with High Open-Circuit Voltages. *Sol. Energy Mater. Sol. Cells* **2009**, *93*, 1688−1691. (c) Dumoulin, F.; Durmuş, M.; Ahsen, V.; Nyokong, T. Synthetic Pathways to Water-Soluble Phthalocyanines and Close Analogs. *Coord. Chem. Rev.* **2010**, *254*, 2792−2847. (d) Li, X.; Jiang, Y.; Xie, G.; Tai, H.; Sun, P.; Zhang, B. Copper Phthalocyanine Thin Film Transistors for Hydrogen Sulfide Detection. *Sens. Actuators, B* **2013**, *176*, 1191−1196. (e) Çimen, Y.; Ermiş, E.; Dumludag, F.; Özkaya, A. R.; Salih, B.; Bekaroglu, Ö. Synthesis, Characterization, Electrochemistry and VOC Sensing Properties of Novel Ball-Type Dinuclear Metallophthalocyanines. *Sens. Actuators, B* **2014**, *202*, 1137−1147. (f) Colomban, C.; Kudrik, E. V.; Afanasiev, P.; Sorokin, A. B. Degradation of Chlorinated Phenols in Water in the Presence of H_2O_2 and Water-Soluble μ-Nitrido Diiron Phthalocyanine. *Catal. Today* **2014**, *235*, 14−19. (g) Matsuzaki, H.; Murakami, T. N.; Masaki, N.; Furube, A.; Kimura, M.; Mori, S. Dye Aggregation Effect on Interfacial Electron-Transfer Dynamics in Zinc Phthalocyanine-Sensitized Solar Cells. *J. Phys. Chem. C* **2014**, *118*, 17205−17212. (h) Arıcan, D.; Erdogmuş, A.; Koca, A. Electrochromism of the Langmuir−Blodgett Films Based on Monophthalocyanines Carrying Redox Active Metal Centers. *Thin Solid Films* **2014**, *550*, 669−676. (i) Melville, O. A.; Lessard, B. H.; Bender, T. P. Phthalocyanine-Based Organic Thin-Film Transistors: A Review of Recent Advances. *ACS Appl. Mater. Interfaces* **2015**, *7* (24), 13105−13118.

(17) (a) Lessard, B. H.; Dang, J. D.; Grant, T. M.; Gao, D.; Seferos, D. S.; Bender, T. P. Bis(tri-*n*-hexylsilyl oxide) Silicon Phthalocyanine: A Unique Additive in Ternary Bulk Heterojunction Organic Photovoltaic Devices. *ACS Appl. Mater. Interfaces* **2014**, *6* (17), 15040−15051. (b) Lim, B.; Bloking, J. T.; Ponec, A.; McGehee, M. D.; Sellinger, A. Ternary Bulk Heterojunction Solar Cells: Addition of Soluble NIR Dyes for Photocurrent Generation beyond 800 nm. *ACS Appl. Mater. Interfaces* **2014**, *6* (9), 6905−6913. (c) Lessard, B. H.; White, R. T.; AL-Amar, M.; Plint, T.; Castrucci, J. S.; Josey, D. S.; Lu, Z.; Bender, T. P. Assessing the Potential Roles of Silicon and Germanium Phthalocyanines in Planar Heterojunction Organic Photovoltaic Devices and How Pentafluoro Phenoxylation Can Enhance $\pi-\pi$ Interactions and Device Performance. *ACS Appl. Mater. Interfaces* **2015**, *7* (9), 5076−5088.

(18) Kane, K. M.; Lemke, F. R.; Petersen, J. L. Bis(trifluoromethanesulfonato)(tetra-p-tolylporphyrinato)silicon(IV), $(TTP)Si(OTf)_2$: The First Structurally Characterized (Porphyrinato)silicon(IV) Complex. *Inorg. Chem.* **1995**, *34* (16), 4085−4091.

(19) A recent publication details the on-surface synthesis of PorSils: Baklanov, A.; Garnica, M.; Robert, A.; Bocquet, M.-L.; Seufert, K.; Küchle, J. T.; Ryan, P. T. P.; Haag, F.; Kakavandi, R.; Allegretti, F.; Auwärter, W. On-Surface Synthesis of Nonmetal Porphyrins. *J. Am. Chem. Soc.* **2020**, *142* (4), 1871−1881.

(20) Liu, J.; Yang, X.; Sun, L. Axial Anchoring Designed Silicon−Porphyrin Sensitizers for Efficient Dye-Sensitized Solar Cells. *Chem. Commun.* **2013**, *49*, 11785−11787.

(21) Yutronkie, N. J.; Grant, T. M.; Melville, O. A.; Lessard, B. H.; Brusso, J. L. Old Molecule, New Chemistry: Exploring Silicon Phthalocyanines as Emerging N-Type Materials in Organic Electronics. *Materials* **2019**, *12* (8), 1334.

(22) Interestingly, while both (i) the exposed hydroxy functionality of the silica gel surface and (ii) methanol form stable bonds to the PorSil to make their respective adducts, attempts to form and isolate the TPP-$Si(OEt)_2$ derivative resulted instead in hydrolysis and the formation of **3**. This suggests that Si−O−C in this porphyrin system is more reactive than Si−Cl in **2**-$SiCl_2$. Attempts to synthesize and observe bulkier alkoxy variants, namely TPP-$Si(O^iPr)_2$ and TPP-$Si(O^tBu)_2$, were also unsuccessful. Also noteworthy to mention is that the bis(trimethylsilyloxy) derivative proved hydrolytically unstable when exposed to the atmosphere and thus was not evaluated in this study. These findings highlight the vital nature of the steric bulk of the axial substituent with respect to the properties of this family of compounds.

(23) As a point of interest, two reduced antiaromatic porphyrin silanes have been synthesized, and in these, the resonances of the protons on the axial substituents are shifted significantly downfield upon coordination: Cissell, J. A.; Vaid, T. P.; Rheingold, A. L. An Antiaromatic Porphyrin Complex: Tetraphenylporphyrinato(silicon)-$(L)_2$ (L = THF or Pyridine). *J. Am. Chem. Soc.* **2005**, *127* (35), 12212−12213.

(24) Vangberg, T.; Ghosh, A. A First-Principles Quantum Chemical Analysis of the Factors Controlling Ruffling Deformations of Porphyrins: Insights from the Molecular Structures and Potential Energy Surfaces of Silicon, Phosphorus, Germanium, and Arsenic Porphyrins and of a Peroxidase Compound I Model. *J. Am. Chem. Soc.* **1999**, *121* (51), 12154−12160.

(25) Planarity can be quantified by evaluating the position of the *meso* carbons of the porphyrin compared to the plane defined by the pyrrole nitrogen atoms; to acquire our data, we established a plane

https://dx.doi.org/10.1021/acs.inorgchem.0c01891
Inorg. Chem. XXXX, XXX, XXX−XXX

defined by N1, Si1, and N2 (i.e., the central silicon and two cis-coordinated porphyrin nitrogen atoms) and measured the shortest distance between this plane and each *meso* carbon. These distances are then averaged to give the common descriptor Δr.

(26) Shelnutt, J. A.; Song, X.-Z.; Ma, J.-G.; Jia, S.-L.; Jentzen, W.; Medforth, C. J. Nonplanar Porphyrins and their Significance in Proteins. *Chem. Soc. Rev.* **1998**, *27* (1), 31−41.

(27) Zheng, J.-Y.; Konishi, K.; Aida, T. Dioxygen Insertion into the Axial Si-C Bonds of Organosilicon Porphyrins. *Chem. Lett.* **1998**, *27* (5), 453−454.

(28) Zheng, J.-Y.; Konishi, K.; Aida, T. Crystallographic Studies of Organosilicon Porphyrins: Stereoelectronic Effects of Axial Groups on the Nonplanarity of the Porphyrin Ring. *Inorg. Chem.* **1998**, *37* (10), 2591−2594.

(29) See paper in ref 23.

(30) Ishida, S.; Yoshimura, K.; Matsumoto, H.; Kyushin, S. Selective Si−C Bond Cleavage on a Diorganosilicon Porphyrin Complex Bearing Different Axial Ligands. *Chem. Lett.* **2009**, *38* (4), 362−363.

(31) Kane, K. M.; Lemke, F. R.; Petersen, J. L. trans-Difluorosilicon(IV) Complexes of Tetra-p-tolylporphyrin and Tetrakis(p-(trifluoromethyl)phenyl)porphyrin: Crystal Structures and Unprecedented Reactivity in Hexacoordinate Difluorosilanes. *Inorg. Chem.* **1997**, *36* (7), 1354−1359.

(32) Observed bond lengths for Si−X in the crystal structure of porphyrin silane (PorSil) and a tetracoordinated (4c) silane (with reference). (a) X = OH, PorSil = 1.67 Å, 4c = 1.66 Å (ref 23). (b) CH_2CH_2, PorSil = 1.83 Å (ref 24), 4c = 1.86 Å: Bartkowska, B.; Krüger, C. Tetravinylsilane. *Acta Crystallogr., Sect. C: Cryst. Struct. Commun.* **1997**, *C53*, 1066−1068. (c) CCPh, PorSil = 1.82 Å (ref 24), 4c = 1.83 Å: Wrackmeyer, B.; Bayer, S.; Tok, O. L.; Klimkina, E. V.; Milius, W.; Kempe, R.; Khan, E. Alkynylsilanes and Alkynyl(vinyl)silanes. Synthesis, Molecular Structures and Multinuclear Magnetic Resonance Study. *Z. Naturforsch., B: J. Chem. Sci.* **2010**, *65* (6), 725−744. (d) CH_2TMS, PorSil = 1.93 Å (ref 24), 4c = 1.92 Å: Buttrus, N. H.; Eaborn, C.; Hitchcock, P. B.; Lickiss, P. D.; Najim, S. T. 1,3 Silicon to Silicon Migration of the Methoxy Group in Solvolysis of (bromodiphenylsilyl)(methoxydimethylsilyl)bis(trimethylsilyl)methane. Crystal Structures of (ethoxydimethylsilyl)(methoxydiphenylsilyl)bis(trimethylsilyl)-methane and (methoxydimethylsilyl)(methoxydiphenylsilyl)bis(trimethylsilylmethane). *J. Chem. Soc., Perkin Trans. 2* **1987**, 1753−1757 As a point of reference, here are two examples for non-planar porphyrins:. (e) Ph, PorSil = 1.94 Å (ref 24.), 4c = 1.86 Å: Párkányi, L.; Sasvári, K. Crystal structure of tetraphenylsilane. Period. Polytechnic. *Chem. Eng.* **1973**, *17* (3), 271−276. (f) F, PorSil = 1.64 Å (ref 26.), 4c = 1.60 Å: Dell, S.; Ho, D. M.; Pascal, R. A. in- and out-Cyclophanes Bearing Non-Hydrogen Bridgehead Substituents. *J. Org. Chem.* **1999**, *64* (15), 5626−5633.

(33) Spackman, M. A.; Jayatilaka, D. Hirshfeld Surface Analysis. *CrystEngComm* **2009**, *11* (1), 19−32.

(34) Charalambidis, G.; Georgilis, E.; Panda, M. K.; Anson, C. E.; Powell, A. K.; Doyle, S.; Moss, D.; Jochum, T.; Horton, P. N.; Coles, S. J.; Linares, M.; Beljonne, D.; Naubron, J.-V.; Conradt, J.; Kalt, H.; Mitraki, A.; Coutsolelos, A. G.; Balaban, T. S. A Switchable Self-Assembling and Disassembling Chiral System Based on a Porphyrin-Substituted Phenylalanine−Phenylalanine Motif. *Nat. Commun.* **2016**, *7* (1), 12657.

(35) Ralphs, K.; Zhang, C.; James, S. L. Solventless Mechanochemical Metalation of Porphyrins. *Green Chem.* **2017**, *19* (1), 102−105.

(36) Valicsek, Z.; Horváth, O. Application of the Electronic Spectra of Porphyrins for Analytical Purposes: The Effects of Metal Ions and Structural Distortions. *Microchem. J.* **2013**, *107*, 47−62.

(37) Uttamlal, M.; Sheila Holmes-Smith, A. The Excitation Wavelength Dependent Fluorescence of Porphyrins. *Chem. Phys. Lett.* **2008**, *454* (4−6), 223−228.

(38) Ghosh, M.; Nath, S.; Hajra, A.; Sinha, S. Fluorescence Self-Quenching of Tetraphenylporphyrin in Liquid Medium. *J. Lumin.* **2013**, *141*, 87−92.

(39) Zheng, W.; Shan, N.; Yu, L.; Wang, X. UV−visible, Fluorescence and EPR Properties of Porphyrins and Metalloporphyrins. *Dyes Pigm.* **2008**, *77*, 153−157.

(40) Chen, Z.; Lohr, A.; Saha-Möller, C. R.; Würthner, F. Self-Assembled π-Stacks of Functional Dyes in Solution: Structural and Thermodynamic Features. *Chem. Soc. Rev.* **2009**, *38* (2), 564−584.

https://dx.doi.org/10.1021/acs.inorgchem.0c01891
Inorg. Chem. XXXX, XXX, XXX−XXX